Bulletin of the Seismological Society of America. Vol. 64, No. 1, pp. 205–219. February 1974

CHARACTERIZATION OF RESPONSE SPECTRA THROUGH THE STATISTICS OF OSCILLATOR RESPONSE

BY F. E. UDWADIA AND M. D. TRIFUNAC

ABSTRACT

This paper presents the physical relationships that exist between the response spectra and the Fourier Transform of strong-motion accelerograms through the extreme value statistics of oscillator response. Under the assumption of a stationary response, it has been shown that the spectrum value depends only on two parameters: a_{rms}, the root-mean-square-value of the response, and, ε, a parameter which measures the distribution of the energy among the various frequencies. The influence of these parameters on the response statistics together with their physical meaning in terms of the oscillator's characteristics have been studied.

Comparisons with the Damped Fourier Transform (Udwadia and Trifunac, 1973) computed velocity spectra and the statistically calculated maximum response are presented for three typical accelerograms. The results indicate that response spectra based on statistical computations lead to good first approximations of the actual response to strong ground motion.

In addition to characterizing the response spectrum with statistical curves expressing the expected value and the most probable value of the peak response, the 5 and 95 per cent confidence levels are also indicated, thus giving the lower and upper bounds for these statistical spectral estimates. These confidence levels delineate the 90 per cent confidence interval.

INTRODUCTION

In recent years, spectrum techniques have gained wide popularity in the analysis and design of earthquake-resistant structures. However, our inability to predict the exact time history of ground motions at a given site has led us to look into the statistical nature of the response of a structure to a stochastic excitation. This paper attempts to correlate the response spectrum of a damped oscillator to the Fourier transform of the input through the statistics of the peaks of the response.

Several researchers have worked on the response of structures to random excitations. However, it has been generally assumed that these excitations are white in character (e.g., Bycroft, 1960; Rosenblueth and Bustamante, 1962; Rosenblueth, 1964). Crandal (1970) has studied the statistics of the time associated with the first passage of an oscillator response above a preset limit. Extensions of the first passage problem to nonstationary excitation have been reported by Corotis *et al.* (1972).

This paper has been motivated by the need for a simple statistical tool for the determination of earthquake response spectra. It attempts to tie in the Damped Fourier Spectrum (Udwadia and Trifunac, 1973), Response Spectra and Fourier transforms with the statistical estimates obtained. The study throws light on the parameters that principally govern the peak response and delineates the extent to which they affect it in a statistical sense. In the discussion that follows, we will assume that the input is a stationary process with an arbitrary power-density function. Although strong shaking is not an ergodic process (and hence the response of an oscillator to it is likewise not ergodic)

(Bogdanoff *et al.*, 1961) in order to highlight the relationships between the Fourier Amplitude Spectrum and the extreme values of the oscillator response, as a first approximation, we will assume that the response can be described adequately by the theory of random ergodic processes. The specific properties of random functions (Rice, 1954) which have been discussed here are related to the distribution of extreme values, the expected values of the maxima in a given time interval and the relationship of these maxima to the rms value of the functions.

The results of the statistical analysis have been applied to the response of an oscillator and the correlations obtained have been discussed in the light of the oscillator's characteristics and the underlying assumptions in the theory.

The distribution of maxima of the maxima of a random function. We begin by summarizing briefly some of the basic results first derived by S. O. Rice (1954) and later extended by Cartwright and Longuet-Higgins (1956). They consider a random function $f(t)$, represented as the sum of an infinite number of sine waves

$$f(t) = \sum_n c_n \cos(\omega_n t + \varphi_n) \tag{1}$$

with frequencies, ω_n, distributed densely in the interval $(0, \infty)$ and phases, φ_n, assumed to be random and uniformly distributed between 0 and 2π. In our applications $f(t)$ will

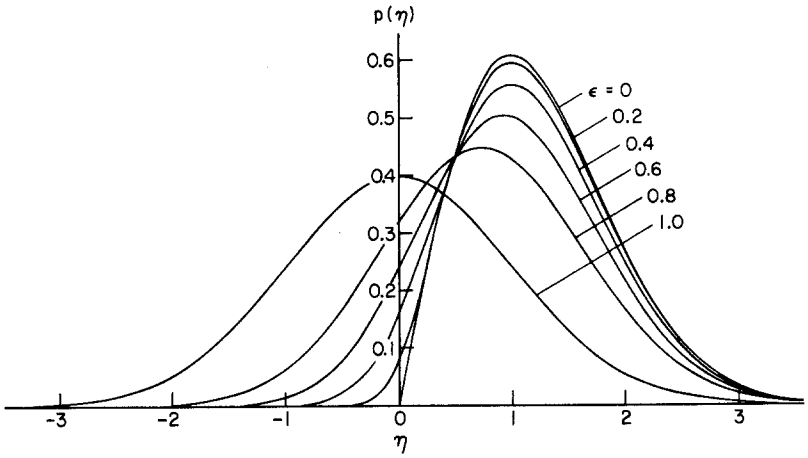

FIG. 1. Graphs of $p(\eta)$, the probability distribution of the heights of maxima for various values of ε.

represent the response of an oscillator to the earthquake ground motion; $E(\omega)$, the energy spectrum of $f(t)$, is related to the amplitudes c_n through

$$\sum_{\omega_n=\omega}^{\omega+d\omega} \tfrac{1}{2}c_n^2 = E(\omega)\, d\omega. \tag{2}$$

The total energy per unit length of the record, corresponding to the first moment of $E(\omega)$ about the origin, is

$$m_0 = \int_0^\infty E(\omega)\, d\omega \tag{3}$$

while the n^{th} moment is defined by

$$m_n = \int_0^\infty E(\omega)\omega^n\, d\omega. \tag{4}$$

Detailed analyses of the statistical distribution of the maxima of $f(t)$ (Cartwright and Longuet-Higgins, 1956) show that this distribution depends on only two parameters:

the root-mean-square value of $f(t,)$ ${m_0}^{1/2}$, and a parameter ε measuring the relative width of the frequency spectrum $E(\omega)$, and defined by

$$\varepsilon^2 = 1 - \frac{{m_2}^2}{m_0 m_4}. \tag{5}$$

From the Cauchy-Schwartz inequality, ε cannot be imaginary.

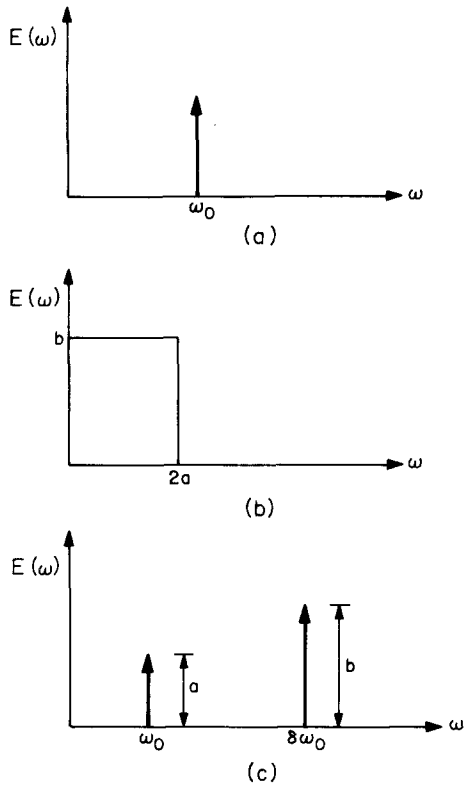

FIG. 2. Three types of energy spectra illustrating the dependence of ε on the shape of the power spectrum.

After normalizing $f(t)$ by

$$f(t)/{m_0}^{1/2} = \eta \tag{6}$$

the probability distribution of the heights of the maxima of $f(t)/{m_0}^{1/2}$ becomes

$$p(\eta) = \frac{1}{(2\pi)^{1/2}}\left[\varepsilon \exp\left(-\frac{1}{2}\frac{\eta^2}{\varepsilon^2}\right) + (1-\varepsilon^2)^{1/2}\eta \exp(-\tfrac{1}{2}\eta^2)\int_{-\infty}^{\eta\frac{(1-\varepsilon^2)^{1/2}}{\varepsilon}} \exp(-\tfrac{1}{2}x^2)dx\right] \tag{7}$$

(Cartwright and Longuet-Higgins, 1956) and is shown in Figure 1. The statistical distribution of the minima is the reflection of (7) in the mean level $\eta = 0$.

Physically, the parameter ε is a measure of the relative proportions of the various frequencies contained in a signal. To fix our ideas on this parameter, let us determine values for the three energy spectra indicated in Figure 2(a, b, c). Figure 2a indicates the spectrum of a pure sine wave. The values of the zeroth, second and fourth moments are

a, $a\omega_0{}^2$, and $a\omega_0{}^4$ so that $\varepsilon = 0$. The corresponding distribution given by equation (7) then reduces to

$$p(\eta) = \begin{cases} \eta \exp(-\frac{1}{2}\eta^2) & \eta \geqq 0 \\ 0 & \eta \leqq 0 \end{cases} \tag{8}$$

showing that for an infinitely narrow spectrum, $p(\eta)$ becomes a Rayleigh distribution.

For the rectangular block shown in Figure 2b, $\varepsilon = 2/3$. The flat nature of the spectrum is indicative of equal proportions of high- and low-frequency contents. Figure 2c indicates two delta functions at frequencies ω_0 and $\delta\omega_0$ of strengths a and b $(=\beta a)$. For such a spectrum

$$\varepsilon^2 = 1 - \frac{(1+\delta^2\beta)^2}{(1+\beta)(1+\delta^4\beta)}$$

the value of ε depends on the relative strengths of the two waves together with their frequency separation. For a fixed $\delta = \delta_0$, if $\beta \to 0$, or $\beta \to \infty$, $\varepsilon \to 0$, and we get the single sine wave case. When, for example, $\delta \to 1/\beta^{1/2}$ and $\beta \to 0$, $\varepsilon \to 1$ thereby indicating a shift towards a Gaussian distribution. The distribution of maxima tends to the distribution of $f(t)/m_0{}^{1/2}$. In this case, we might expect equal numbers of positive and negative maxima of $f(t)/m_0{}^{1/2}$ and, therefore, a $p(\eta)$ symmetric about $\eta = 0$. Indeed, setting $\varepsilon = 1$ in (7) we obtain

$$p(\eta) = (2\pi)^{-1/2} \exp(-\tfrac{1}{2}\eta^2) \tag{9}$$

which is the Gaussian distribution. For values of ε between 0 and 1, $p(\eta)$ lies between the Rayleigh and Gaussian distributions as shown in Figure 1.

An example in Figure 3 illustrates how ε measures the relative width of the power spectrum of the response of a single-degree-of-freedom system to a stationary excitation having a power spectrum given by

$$\Phi(\omega) = \frac{1}{1+\left(\frac{\omega}{\alpha}\right)^2}. \tag{10}$$

The transfer function of a single-degree-of-freedom system is given by

$$H(\omega) = \frac{1}{\omega_n{}^2 - \omega^2 - 2i\omega_n\xi\omega} \tag{11}$$

where ω_n is the natural frequency of the oscillator and ξ is the fraction of critical damping. The dimensionless parameter

$$\zeta = \frac{\alpha}{\omega_n} \tag{12}$$

is a measure of the width of the input spectrum relative to the natural frequency of the oscillator considered. Figure 3 then shows that when ξ, the fraction of critical damping, tends to zero, i.e., when the peak of the transfer function $H(\omega)$ at $\omega = \omega_n$ becomes sharper and higher, the oscillator becomes increasingly more sensitive only to the input frequencies $\omega \approx \omega_n$ and the output spectrum reduces to a narrow band centered at $\omega = \omega_n$ with $\varepsilon \ll 1$. In the other extreme case, when $\xi \to 1$ the oscillator "feels" all frequencies between 0 and ω_n equally well, the output spectrum broadens and $\varepsilon \to 1$. In addition to this effect of ξ, the influence of the cut-off frequency α of the input spec-

trum on ε, also shown in Figure 3, demonstrates that for the broad-band excitation only small ξ leads to a "narrow" output spectrum as measured by ε.

The expected value and the most probable value of the maximum wave amplitude. Let the peaks of the function $f(t)$ be denoted by $a_1, a_2, \ldots a_n$, the rms value of $f(t)$ be denoted by a_{rms} and let $\bar{a}$ denote $\sqrt{2}a_{\text{rms}}$. $\bar{a}$ may then be interpreted as the rms value of the peak amplitudes when $f(t)$ is a narrow-band process (i.e., ε is small) (Udwadia and Trifunac, 1973).

The probability distribution of $a_{\max}$, the maximum wave amplitude, can then be derived by assuming that the sampling of the peak amplitudes is at random. Strictly, this assumption does not hold, since the sample consists of N consecutive peaks bounded by a slowly fluctuating amplitude, and there must be some correlation between the consecutive peaks especially when the power spectrum of $f(t)$ is narrow. However, as pointed out by Longuet-Higgins (1952), fluctuations of the envelope function may act as a "randomizing" process leading to a better agreement between the observed and theoretical distributions.

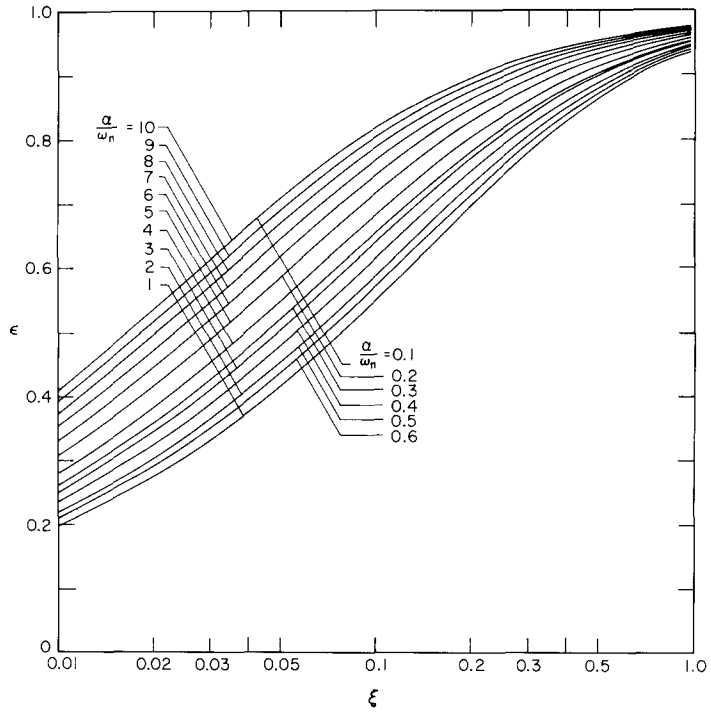

FIG. 3. Graph of ε as a function of the percentage of critical damping, ξ, of a single-degree-of-freedom system subjected to the band limited (from 0 to α radians/sec) signal $\Phi(\omega)$.

It can be shown that the expected value for $\varepsilon = 0$ is given by

$$\frac{E(a_{\max})}{\bar{a}} = \frac{\sqrt{\pi}}{2}\left(N - \frac{N(N-1)}{2!\sqrt{2}} + \frac{N(N-1)(N-2)}{3!\sqrt{3}} + \ldots(-1)^{N+1}\frac{1}{\sqrt{N}}\right) \tag{13}$$

(Longuet-Higgins, 1952) where N is the number of waves considered in the sample. The asymptotic form of equation (13) for large N becomes

$$\frac{E(a_{\max})}{\bar{a}} \approx (lnN)^{1/2} + \tfrac{1}{2}\gamma(lnN)^{-1/2} \tag{14}$$

where γ is Euler's constant equal to 0.5772. The difference between the expressions on the right-hand sides of equations (14) and (13) is of order $(lnN)^{-3/2}$ and does not affect the approximate result even for small values of N (Udwadia and Trifunac, 1973).

The most probable peak amplitude, designated by $\mu(a_{\max})$, can be approximated by

$$\frac{\mu(a_{\max})}{\bar{a}} \approx [lnN]^{1/2} \tag{15}$$

(Longuet-Higgins, 1952).

For nonzero values of ε, equation (14) becomes

$$\frac{E(a_{\max})}{\bar{a}} \approx [ln(1-\varepsilon^2)^{1/2}N]^{1/2} + \tfrac{1}{2}\gamma[ln(1-\varepsilon^2)^{1/2}N]^{-1/2} \tag{16}$$

and is valid only when $(1-\varepsilon^2)^{1/2}N$ is large (Cartwright and Longuet-Higgins, 1956). Although the above expression is strictly invalid for $\varepsilon \to 1$, the results obtained from equation (16) for $\varepsilon = 0.990$ do not differ appreciably from Tippett's (1925) exact results for values of $N > 3$ (Udwadia and Trifunac, 1973). As $\varepsilon \to 0$ (16) reduces to (14). Figure 4 and Table 1 give the values of $E(a_{\max})/\bar{a}$ for $\varepsilon = 0$, 0.2, 0.4, 0.6, and 0.8 derived

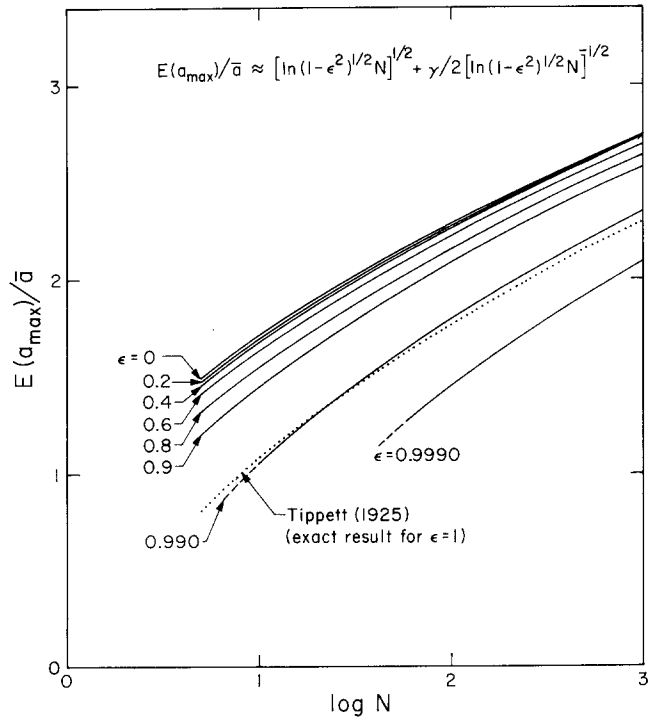

FIG. 4. Asymptotic approximation for the expected peak value $E(a_{\max})$ when $(1-\varepsilon^2)^{1/2}N$ is large.

from (16). From this Figure, we observe that the value of $E(a_{\max})/\bar{a}$ does not vary appreciably with either N or ε. The most critical factor then in the determination of $E(a_{\max})$ is the value of $\bar{a}$. Damping in the system has two effects; it changes the rms of the response, which is related to the energy in the oscillations, and it affects the value of ε, which is related to the distribution of this energy among the different frequencies.

The lower and upper bound confidence levels for $a_{\max}$. Here we consider the probability

of a_{max} exceeding a given level, with the objective of calculating an estimate of the lower and upper bounds of a_{max} that depend on N and the preselected probability that a_{max} will not exceed it. We choose to call these curves "the lower and upper bound confidence levels" and designate them by $a_{MIN,\,1-C}$ and $a_{MAX,\,C}$, where C specifies the confidence level selected. These two curves, calculated for the various oscillator frequencies ω_n, then delineate a region between them which we will call the "90 per cent Confidence Interval" (Figures 7–10).

The probability that a_{max} will exceed a given level r, for $\varepsilon = 0$, is given by

$$p(r) = \int_r^\infty d[(1-\exp(-r^2/\bar{a}^2))^N]$$
$$= 1-(1-\exp(-r^2/\bar{a}^2))N$$

(Udwadia and Trifunac, 1973).

TABLE 1

VALUES OF $E(a_{max})/\bar{a}$ AS A FUNCTION OF ε

N	$E(a_{max})/\bar{a}$						
	$\epsilon^* = 0$	$\epsilon^* = 0.2$	$\epsilon^* = 0.4$	$\epsilon^* = 0.6$	$\epsilon^* = 0.8$	$\epsilon^* = 0.990$	$\epsilon\dagger = 1.0$
5	1.496	1.490	1.468	1.423	1.323	—	0.822
10	1.708	1.701	1.682	1.642	1.554	1.079	1.088
20	1.898	1.892	1.875	1.838	1.759	1.301	1.321
50	2.124	2.119	2.103	2.071	2.001	1.604	1.587
100	2.280	2.276	2.261	2.231	2.166	1.804	1.773
200	2.427	2.423	2.409	2.381	2.320	1.985	1.942
500	2.609	2.605	2.592	2.565	2.509	2.203	2.147
1000	2.738	2.734	2.722	2.697	2.643	2.354	2.292

*Approximation (16).
†Exact (Tippett, 1925).

By defining r_o by the equation

$$r_o^2/\bar{a}_o^2 = lnN;\ \exp(-r_o^2/\bar{a}^2) = 1/N$$

it can be shown that

$$\frac{d}{dr}\left[1-\frac{1}{N}\exp\left(\frac{r_o^2-r^2}{\bar{a}^2}\right)\right]^N \approx \frac{d}{dr}\exp\left[-\exp\left(\frac{r_o^2-r^2}{\bar{a}^2}\right)\right].$$

The upper bound confidence level $a_{MAX,\,C}$ then becomes the solution of the equation

$$1-(1-\exp(-a^2{}_{MAX,\,C}/\bar{a}^2))^N = 1-C. \tag{18}$$

Solving for $a_{MAX,\,C}/\bar{a}$ we obtain

$$\frac{a_{MAX,\,C}}{\bar{a}} = [-ln(1-C^{1/N})]^{1/2}. \tag{19}$$

Mutatis mutandis in (18) and (19) the result for $a_{MIN,\,1-C}$ follows immediately. Ten different $a_{MAX,\,C}/\bar{a}$ and $a_{MIN,\,(1-C)}$ curves for C ranging from 0.90 to 0.99 are compared with the $E(a_{max})/\bar{a}$ curve for $\varepsilon = 0$ in Figure 5. Both $a_{MAX,\,C}/\bar{a}$ and $a_{MIN,\,1-C}/\bar{a}$ are tabulated in Table 2 for $C = 0.90, 0.95$, and 0.99.

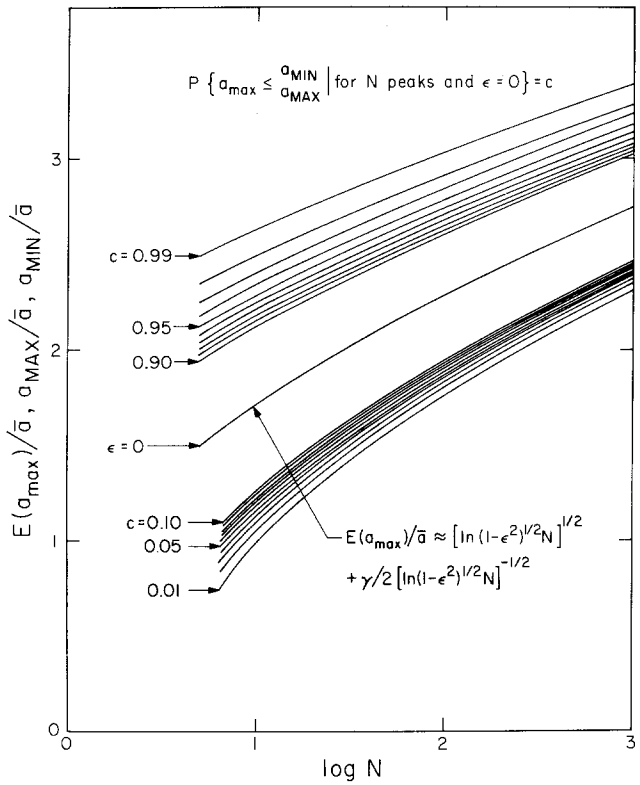

FIG. 5. Upper and lower bounds for a_{max} for different confidence levels plotted versus the logarithm of the number of peaks.

TABLE 2

VALUES OF $a_{MAX,\ c/\bar{a}}$ AND $a_{MIN,\ 1-c/\bar{a}}$

N	$a_{MAX,\ c/\bar{a}}$	$a_{MIN,\ 1-c/\bar{a}}$	C
1	2.146	0.100	
10	2.627	0.998	
100	3.034	1.761	0.99
1,000	3.392	2.320	
10,000	3.715	2.772	
1	1.731	0.226	
10	2.297	1.163	
100	2.752	1.877	0.95
1,000	3.143	2.411	
10,000	3.490	2.848	
1	1.517	0.325	
10	2.135	1.258	
100	2.618	1.945	0.90
1,000	3.026	2.464	
10,000	3.385	2.894	

Applications to response spectrum analysis. The response of an oscillator subjected to an input ground motion $-\ddot{z}(t)$ can be obtained in frequency space as the product of the transfer function of the oscillator and the Fourier transform of $\ddot{z}(t)$. It shall be assumed

in what follows that the oscillator started from rest. Hence

$$R(\omega) = H(\omega)Z(\omega),$$

where $H(\omega)$ is the transfer function of the oscillator, $Z(\omega)$ is the transform of the input function, and $R(\omega)$ is the response.

As seen from the previous section, the two parameters which influence the response of such an oscillator are ε, which is a measure of the distribution of energy among the various frequencies, and a_{rms}, which is a measure of the total energy of the system. The computation of a_{rms} can be done in terms of the values of $H(\omega)$ and $Z(\omega)$ as follows

$$a_{\text{rms}}^2 = \frac{1}{T}\int_0^T r^2(t)dt = \frac{1}{2\pi T}\int_{-\infty}^{\infty} |R(\omega)|^2 \, d\omega = \frac{1}{2\pi T}\int_{-\infty}^{\infty} |H(\omega)|^2 |Z(\omega)|^2 \, d\omega \tag{20}$$

$$a_{\text{rms}}^2 = \frac{1}{\pi T}\int_0^{\infty} |H(\omega)|^2 |Z(\omega)|^2 \, d\omega. \tag{21}$$

This can be easily calculated for any given input and any desired oscillator transfer function $H(\omega)$. The corresponding values of ε can then be calculated by computing the zeroth, second, and fourth moments of $|R(\omega)|$.

Next an estimate of the total number of maxima, N, is required. We shall assume here that the oscillator acts as a narrow-band filter and that the value of N can be taken as the ratio of the duration of the record and the fundamental period τ of the oscillator. A knowledge of these parameters enables the calculation of the expected value of the most probable peak [equation (15)], the expected value of the maximum peak [equation (16)], and the lower and upper bound confidence levels [equation (19)].

Statistics on the pseudo velocity can be obtained by multiplying by ω each of the three quantities statistically determined. Statistics on the velocity spectrum are generated by considering the function $|\omega R(\omega)|^2$ instead of $|R(\omega)|^2$ in equation (20). Here we present the results for the true velocity spectrum only (Udwadia and Trifunac, 1973).

A case study on three accelerograms. The statistical approach outlined above is based on a large number of assumptions; therefore, the applicability of the method to give suitable approximations of the velocity and pseudo velocity spectra was checked using three different types of real accelerograms. The first accelerogram used was the Eureka 1954 record shown in Figure 6a. The acceleration consists of a short burst of energy about 5 sec long preceded and followed by much smaller motions. Figure 7 shows the velocity spectrum curves. The lowermost curve is the Damped Fourier Spectrum (Udwadia and Trifunac, 1973) drawn for 2 per cent damping, while the statistical curves are indicated by dashed and dotted lines. The calculated true velocity spectrum ($\xi = 0.02$) is shown by full circles. The length of record analyzed was 20 sec.

We note that the Damped Fourier Spectrum curve ($\xi = 0.02$) is below the velocity spectrum points (full circles) ($\xi = 0.02$). This is exactly what we would expect since the amplitude of the D.F.S. is related to the velocity and displacement of the oscillator at the end of the excitation (Udwadia and Trifunac, 1973) and is therefore always less than or equal to the true velocity spectrum. These damped spectral curves can then also be used as lower bounds for the damped velocity spectra. Statistical curves for frequencies below 2 Hz show good correlations with the computed velocity spectra. However, at higher frequencies rather large divergences (5–10 per cent) occur. This is caused by the nonstationary nature of the excitation. The lack of high-frequency contents in the signal tends to reduce the scaling factor, $\bar{a}$, when averages over longer time lengths are taken. However, we observe that the general trends in the statistical curves do follow the trends in the velocity spectrum.

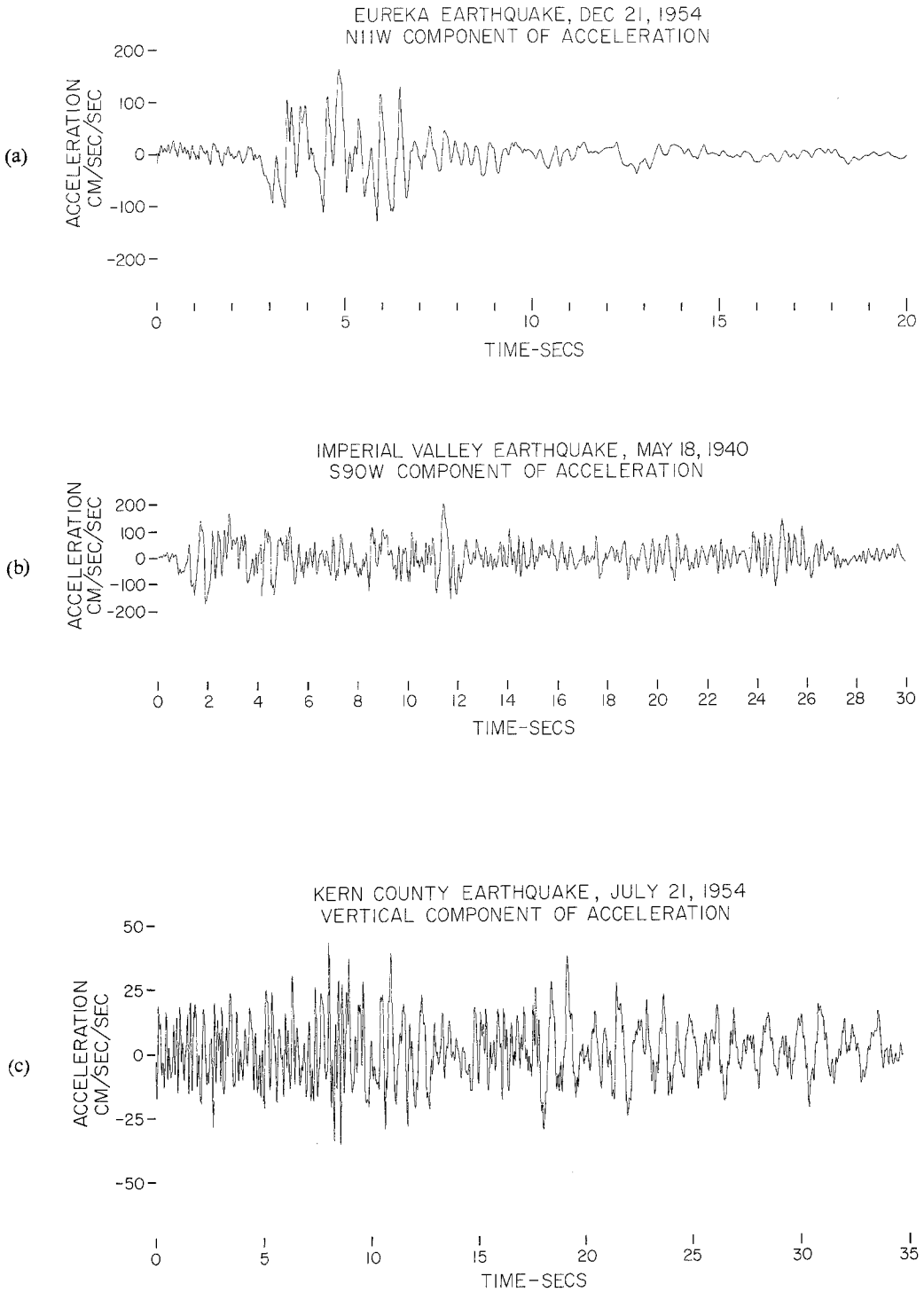
(a)
EUREKA EARTHQUAKE, DEC 21, 1954
N11W COMPONENT OF ACCELERATION
ACCELERATION CM/SEC/SEC
200
100
0
-100
-200
0
5
10
15
20
TIME-SECS
(b)
IMPERIAL VALLEY EARTHQUAKE, MAY 18, 1940
S90W COMPONENT OF ACCELERATION
ACCELERATION CM/SEC/SEC
200
100
0
-100
-200
0
2
4
6
8
10
12
14
16
18
20
22
24
26
28
30
TIME-SECS
(c)
KERN COUNTY EARTHQUAKE, JULY 21, 1954
VERTICAL COMPONENT OF ACCELERATION
ACCELERATION CM/SEC/SEC
50
25
0
-25
-50
0
5
10
15
20
25
30
35
TIME-SECS

FIG. 6.

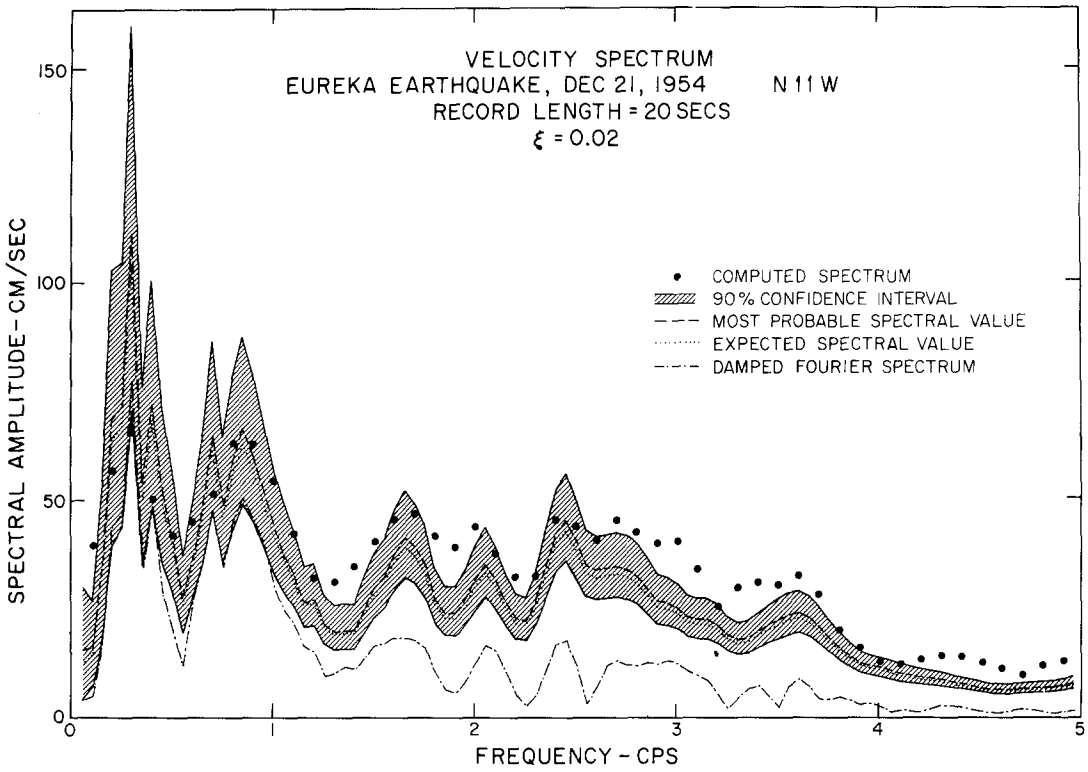

FIG. 7. The velocity spectrum, the Damped Fourier Spectrum, and the statistical estimates for a 20-sec length of the Eureka accelerogram (Figure 6a).

To study this point further, 2 per cent damping curves were calculated for the first 10 sec of the record (Figure 8). We observe an improved correlation between the statistical bounds and the calculated spectral values up to about 4 Hz.

The next accelerogram tested was the El Centro event of 1940. The curves corresponding to a 30-sec length of this accelerogram (Figure 6b) show a good correlation all the way to 5 Hz (Figure 9). The nearly stationary response of a lightly damped oscillator to this acceleration history makes the statistical estimates excellent indications of the true spectral values.

The third accelerogram tested was the Kern County accelerogram (Figure 6c). This accelerogram is representative of a large number of real accelerograms in that it starts off with the high-frequency arrivals (*S* and *P* waves) and carries on with the various surface-wave modes. As we go along the accelerogram, the frequency content changes, there being less and less higher-frequency components in the surface-wave arrivals. Thirty-five seconds of record were analyzed, and the 2 per cent damped spectrum is obtained as shown in Figure 10. The figures show that up to about 1.8 Hz the spectral points (full circles) are pretty much straddled by the 90 per cent confidence interval. At higher frequencies again, a noticeable fall-off in the statistical values occurs. The maximum difference between the statistically expected maxima and the actual spectral values is about 20 per cent.

The above three accelerograms have been chosen as representatives of a large number of real accelerograms obtained during strong ground shaking. The results indicate that statistical studies can be made very fruitfully if we consider lengths of record which are

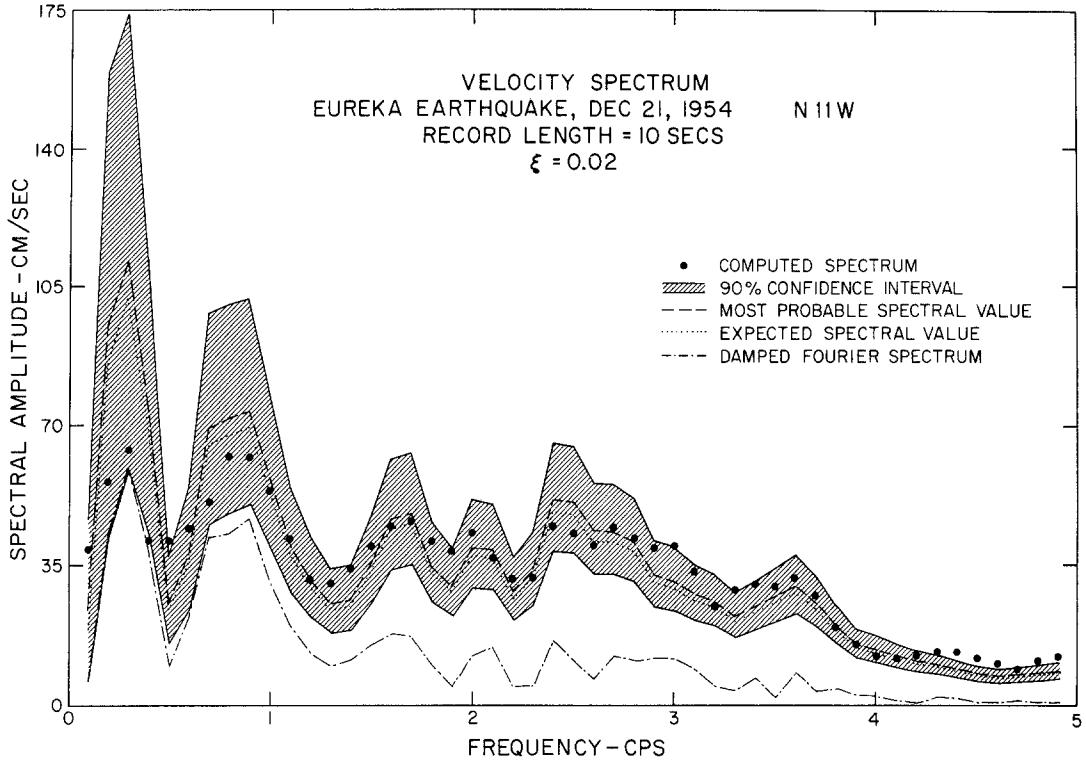

FIG. 8. The velocity spectrum, the Damped Fourier Spectrum, and the statistical estimates for a 10-sec length of the Eureka accelerogram (Figure 6a).

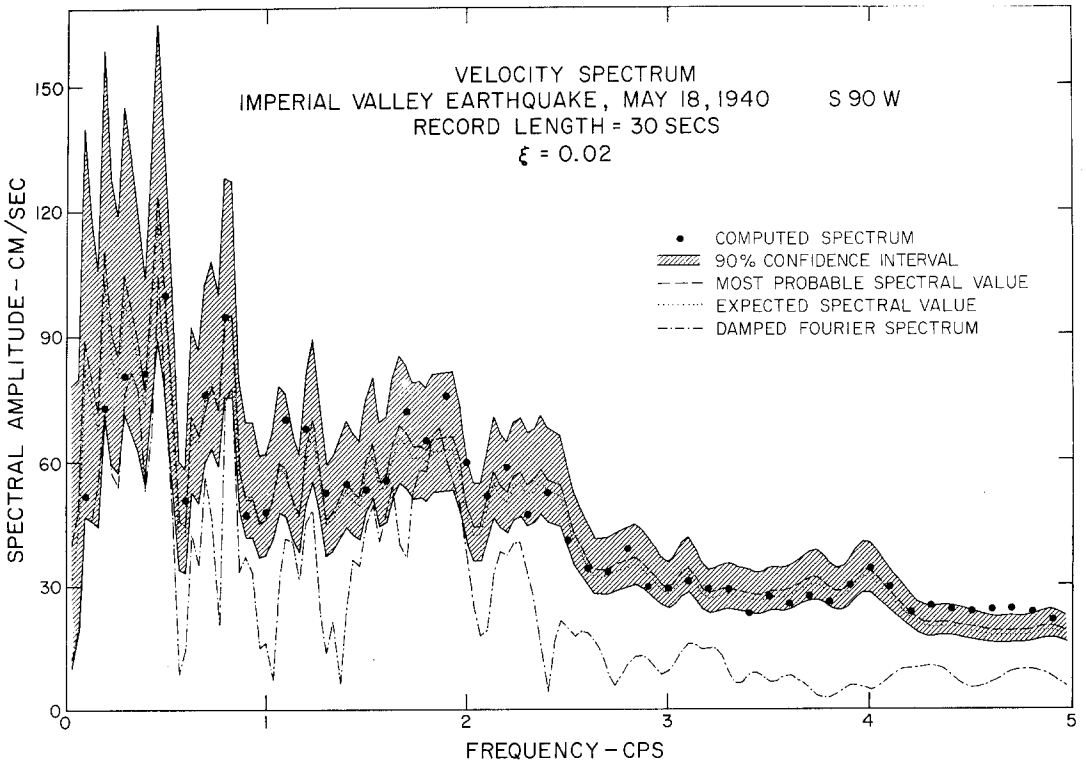

FIG. 9. The velocity spectrum, the Damped Fourier Spectrum, and the statistical estimates for a 30-sec length of the El Centro accelerogram (Figure 6b).

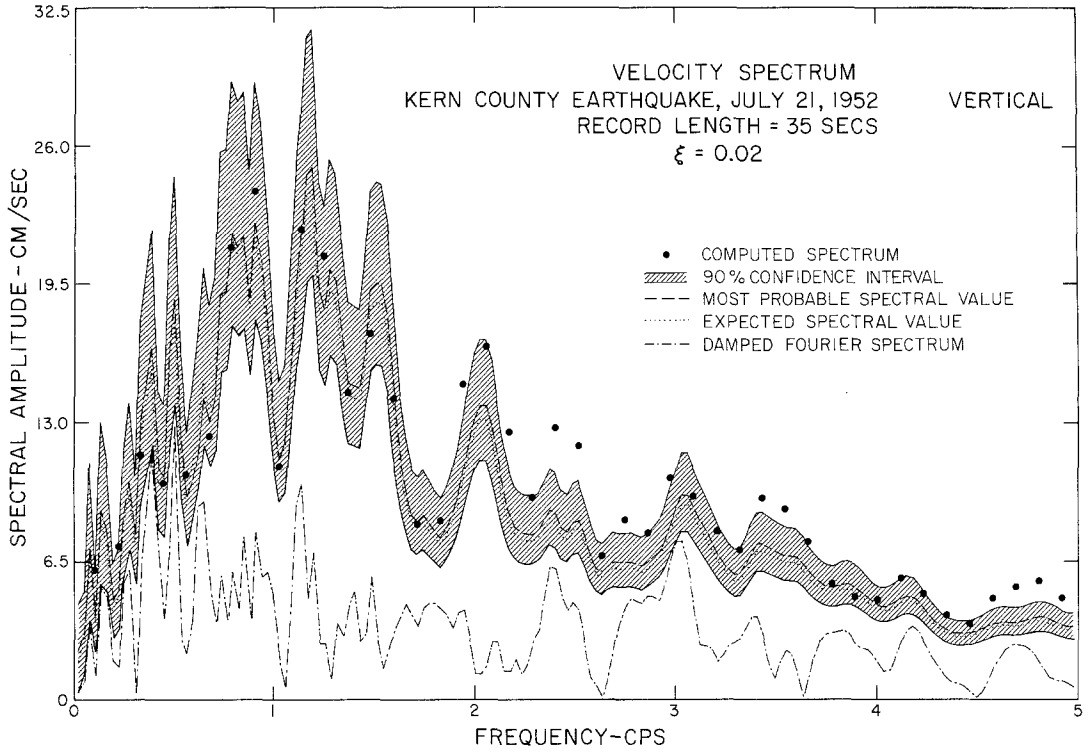

FIG. 10. The velocity spectrum, the Damped Fourier Spectrum, and the statistical estimates for a 35-sec length of the Kern County accelerogram (Figure 6c).

nearly stationary with respect to the frequencies of interest to us. The fact that the higher frequency components die out earlier in the record necessitates a shorter time segment of record for statistical analysis of real accelerograms to get better estimates at higher frequencies, than would be generally required for longer periods. However, the lengths of the record analyzed should contain a sufficiently large number of cycles (at least 4 or 5) of the oscillator so as to make such a statistical approach meaningful.

DISCUSSION

At frequencies below 1 Hz, the statistical estimates tend to be above the actual computed values. Studies on white noise excitation indicate that this may be principally attributed to the numerical errors in integration which arise when the transfer function $H(\omega)$ is peaked around zero frequency (Udwadia and Trifunac, 1973). These errors tend to overestimate the area expressed by equation (21). In order to minimize this error, the Fourier transform was linearly interpolated between two consecutive frequency estimates and the area then computed. A better method would be the use of the sampling theorem to define $Z(\omega)$ continuously and then an integration of the product $Z(\omega)H(\omega)$. Also, it must be remembered that statistical estimates for values of N which are less than 2 or 3 may not be meaningful, for the analysis assumes that the time length of record is long enough to ensure that the sample of wave heights is sufficiently representative. As observed by Corotis *et al.*, (1972), this lack of stationarity may lead to lower response spectrum values than those determined by the statistical analysis under the stationary assumption.

In addition to the overestimation of the spectral amplitudes at lower frequencies ($N \leqq 4$), other errors arise in dealing with real accelerograms. Here the major problem is the lack of stationarity of the data. At any given site, the motions created by an earthquake indicate the arrivals of various phases at various times. Characteristically, the S and P waves which arrive early in the complete time history show larger portions of higher-frequency contents than the later arrivals of the longer-period surface waves. A proper statistical analysis based on the assumption of stationarity would then require that the time length of recording chosen not be too long, so that in this time the frequencies and amplitudes do not change significantly. This has already been illustrated through the study of two different time lengths of the Eureka earthquake record (Figures 7 and 8).

The damping ratio also affects ε. Larger damping ratios will generally lead to larger ε's and broader-band processes (Udwadia and Trifunac, 1973). Although the most probable level and the confidence level curves shown in all of the figures correspond to values of $\varepsilon = 0$, they can be used as conservative upper bounds for $\varepsilon \neq 0$, since these curves for $\varepsilon = 0$ will cause an overestimation of the spectral estimates.

Conclusions

It has been illustrated that given the Fourier transform of the input ground motion $\ddot{z}(t)$, statistical estimates of the maximum response of any single-degree-of-freedom linear system can be easily determined if the assumption of stationarity is approximately satisfied. The two parameters of importance are the relative distribution of energy among the various frequencies and the rms level. These parameters depend on the nature of the input spectrum and on the damping ratio of the oscillator. Larger damping ratios cause relatively wider response energy spectra and hence lead to increased values of ε. Typically, for most earthquakes, the values of ε tend to be between about 0.2 and 0.5. When $\varepsilon \to 0$, we get to a pure sinusoid while with $\varepsilon \to 1$, $p(\eta)$ tends to a Gaussian distribution.

Although the assumption of stationarity is far from correct in dealing with real accelerograms, it has been demonstrated that with a judicious choice of the record duration, estimates of the damped spectra to within 10 to 15 per cent of the true values can be easily obtained. The success of the statistical method is greatly due to its relative insensitivity to factors such as the estimated number of waves and the spectral width ε. Its strong dependence on the rms level is, however, a serious limitation in that it requires a careful choice of the time length needed to simulate stationary conditions.

Acknowledgments

This research was supported in part by grants from the National Science Foundation and the Earthquake Research Affiliates Program at the California Institute of Technology.

References

Bycroft, G. N. (1960). White noise representation of earthquakes, *Proc. Am. Soc. Civil Eng.* **86,** EM2, 1–16.

Bogdanoff, J. L., J. E. Goldberg, and M. C. Bernard (1961). Response of a simple structure to a random earthquake-type disturbance, *Bull. Seism. Soc. Am.* **51** (2), 293–310.

Cartwright, D. E. and M. S. Longuet-Higgins (1956). The statistical distribution of maxima of a random function, *Proc. Roy. Soc. London, Ser. A* **237,** 212–232.

Corotis, R. B., E. H. Vanmarcke, and C. A. Cornell (1972). First passage of nonstationary random processes, *Proc. Am. Soc. Civil Eng.* **98,** EM2, 401–414.

Crandal, S. H. (1970). First-crossing probabilities of the linear oscillator, *J. Sound Vibr.* **12,** 285–300.

Longuet-Higgins, M. S. (1952). On the statistical distribution of the heights of sea waves. *J. Marine Res.* **3,** 245–266.

Rice, S. O. (1954). Mathematical analysis of random noise, in *Selected Papers on Noise and Stochastic Processes,* Nelson Wax, Editor, Dover, N.Y.

Rosenblueth, E. and J. I. Bustamante (1962). Distribution of structural response to earthquakes, *Proc. Am. Soc. Civil Eng.* **88,** EM3, 75–106.

Rosenblueth, E. (1964). Probabilistic design to resist earthquakes, *Proc. Am. Soc. Civil Eng.* **90,** EM5, 189–219.

Tippett, L. H. C. (1925). On the extreme individuals and the range of samples taken from a normal population, *Biometrika* **17,** 364–387.

Udwadia, F. E. and M. D. Trifunac (1973). Fourier transforms, response spectra and their relationship through the statistics of oscillator response, *EERL 73-01,* Earthquake Eng. Res. Lab., California Institute of Technology.

EARTHQUAKE ENGINEERING RESEARCH LABORATORY
CALIFORNIA INSTITUTE OF TECHNOLOGY
PASADENA, CALIFORNIA 91109

Manuscript received May 4, 1973